Power Frequency Control Method of Electrical Equipment Under Internet of Things Technology

Hong-yu Huang(✉) and Qing-huan Qin

Guangxi Modern Polytechnic College, Hechi 547000, China
huanghongyu6542@163.com

Abstract. The power frequency of electrical equipment is related to the safety of the equipment, but the traditional control method is difficult to guarantee the safety of the electrical equipment because of the small difference between the activity characteristics of the power information extracted by the traditional control method. Therefore, this study proposes a power frequency control method for electrical equipment based on Internet of Things technology. Firstly, power supply information of electrical equipment is collected based on the Internet of Things technology, and then a collaborative model is established to extract the frequency fluctuation characteristics of power supply. Based on this, the frequency fluctuation range is located, the node information is compressed sensing on the basis of two feature data processing, and then chaotic algorithm is used to control the frequency fluctuation trajectory of the power supply. Four groups of variables were set to test the safety performance guarantee effect of the control method. Compared with the traditional control method, the safety factor of the electrical equipment is 7.96% higher than that of the traditional control method. It can be seen that the method in this paper can effectively improve the use safety of electrical equipment.

Keywords: Internet of Things technology · Electrical equipment · Power frequency control · Safety factor

1 Introduction

With the rise of network science and technology, foreign countries first began to study signal transmission control theory through mathematical abstract hypotheses in 1736. After that, for nearly two centuries, people have been combining mathematical abstract hypotheses to control the synchronous transmission of signals. The domestic research on this work started late, but with the continuous deepening and innovation of various science and technology, various synchronous control strategies or methods have different research progress. Among them, in reference [1], a 5 kHz high-frequency ice-melting excitation power supply is designed to achieve large-capacity output of the system through parallel inverter modules, and then the drive signal of the inverter switch is generated by carrier phase shift technology to reduce the working frequency of the switch, so as to improve the control effect of the output frequency of the power supply. In Reference [2], on the basis of determining the power frequency control range

S. Wang et al. (Eds.): IoTCare 2021, LNICST 414, pp. 526–541, 2022.
https://doi.org/10.1007/978-3-030-94185-7_35

of the power electronic interface, the equivalent inertia and the difference adjustment coefficient of the power system are calculated, and then the frequency control of the power system is realized through the frequency support between multi-synchronous networks.

On the basis of the above research, this paper combines the existing frequency control technology of different objects to carry out optimization research on the power frequency control of electrical equipment. The main work of this paper is as follows:

(1) Collect power supply information of electrical equipment based on Internet of Things technology and establish a collaboration model, so as to extract frequency fluctuation characteristics of power supply.
(2) By positioning the frequency fluctuation range, and on the basis of two characteristic data processing, compressed sensing node information is used, and then chaos algorithm is used to control the power frequency fluctuation trajectory, so as to realize the effective control of power frequency.

2 Method Design

2.1 Collect Electrical Equipment Power Information Based on the Internet of Things Technology

The Internet of Things technology includes information collection technology, wireless network communication technology, wireless positioning technology, and smart technology. The Internet of Things technology is used to monitor the power supply of electrical equipment. The Internet of Things RFID sensor technology uses TDOA (Time Difference of Arrival Algorithm) to obtain the activity status of electrical equipment in different cycles according to the hyperbola [3, 4]. Assuming that A, B, C, and D represent the position of the RFID reader, it is known that the position coordinates are statically fixed. Set E to represent the position of the node that needs to be located. The TDOA algorithm uses points AB and CD to create a hyperbola. When point P is within the radio frequency range of the radio frequency reader, the following formula is used to calculate the position coordinates of point P.

$$\begin{cases} W_{AB} = t_1 v = |PA - PB| \\ W_{CD} = t_2 v = |PD - PC| \end{cases} \tag{1}$$

In the formula: W_{AB} and W_{CD} respectively represent the distance difference between point P to point A and point B; t_1 and t_2 represent the time difference between the radio frequency signal at point P and point A and B respectively; v represents the signal transmission speed; PA, PB, PD, PC represent the distance between point P and the RFID reader. Bring the calculation result of the above formula into the hyperbolic formula to calculate the position coordinates of the P point. The equation is:

$$\begin{cases} R_{AB} = \sqrt{(X_A - X)^2 + (Y_A - Y)^2} - \sqrt{(X_B - X)^2 + (Y_B - Y)^2} \\ R_{CD} = \sqrt{(X_C - X)^2 + (Y_C - Y)^2} - \sqrt{(X_D - X)^2 + (Y_D - Y)^2} \end{cases} \tag{2}$$

In the formula: (X_A, Y_A), (X_B, Y_B), (X_C, Y_C), and (X_D, Y_D) represent the coordinates of points A, B, C, and D respectively, and (X, Y) is the coordinates of point P for calculation. Solve the above formula and calculate the specific (X, Y) value [5, 6]. After the Internet of Things technology collects electrical equipment power information, it uploads the information to the control platform, and uses the platform's correlation analysis and linkage operation functions to transform the island information that was originally in an isolated state into linkage information.

2.2 Establish a Collaborative Model to Extract the Characteristics of Power Frequency Fluctuations

On the premise of the integration of the digital control platform and the Internet of Things technology, according to the collaborative mechanism of the Internet of Things and electrical equipment, a collaborative model is established to extract the characteristics of power frequency fluctuations. Assuming that the operational risk of the control platform is neutral, and the various data in the platform can be regarded as a single mechanism of approximate project discrete changes, a two-state model of binomial distribution conforming to a single period is created. In the basic management module of electrical equipment, considering the flexibility of the control program, it is assumed that the decision maker adjusts the original operation plan according to the actual operating conditions of the electrical equipment within a certain period of time [7]. Assuming that the value-added amount is M, the risk probability when the platform is used at this time is:

$$o = \frac{t_i}{t_0} \times R(n + \varepsilon) \tag{3}$$

In the formula: o represents the risk probability; t_i represents the power data adjustment time in the i period; t_0 represents the initial time of the dynamic change of the power data; n represents the original data volume; ε represents the increased or decreased data volume after adjustment using t_1, t_2, t_3 respectively represents different equipment operating periods. According to the change probability of power-related data, a collaborative analysis model is established:

$$K = e^{-k}[o \times (\varphi a + \delta) + (1 - o) \times (\varphi b + \delta)] \tag{4}$$

In the formula: e represents the risk identification coefficient; k represents the risk indicator; φ represents the volatility value of the platform; a represents the rate of increase in risk; b represents the rate of decrease in risk. Use the model to mine and analyze the data characteristics of the electrical equipment power information, compare the results with the actual data characteristics, and find out the related parts between the

two. Using grid fast density clustering algorithm, the electrical equipment power data information is divided into several adjacent intervals according to the dimensions, and a set composed of grid cells is established. A dynamic two-dimensional array is used to access the entire data set. Unordered data sets are transposed into an ordered structure in a specific space to achieve clustering of data. The data space in the data set is divided by the method of equal width division [8]. Assuming that the two-dimensional data object is u, and its neighborhood is centered at u and r is the radius, the collection of all data objects forms a single data set. Therefore, it is appropriate to set the width of the grid to be a value. Suppose the two-dimensional data set is Z, its attribute is (U, V), the values of U and V dimensions are $(u_{\min}, u_{\max})$, $(v_{\min}, v_{\max})$, and r is the grid width for division, and the specific number of grids obtained is:

$$\begin{cases} U = \left(\dfrac{u_{\max} - u_{\min}}{r}\right) \\ V = \left(\dfrac{v_{\max} - v_{\min}}{r}\right) \end{cases} \tag{5}$$

The number of grids in each dimension takes an integer value upwards. Read the data set Z and divide it into a grid of $U \times V$. After the grid unit corresponding to each list is initialized, the power supply data of electrical equipment is read into the memory, and the attribute characteristics are calculated by the allocation function according to the actual spatial position, and then placed into the corresponding grid. At this time, there are many types of data features mined. The power data feature types are shown in Fig. 1.

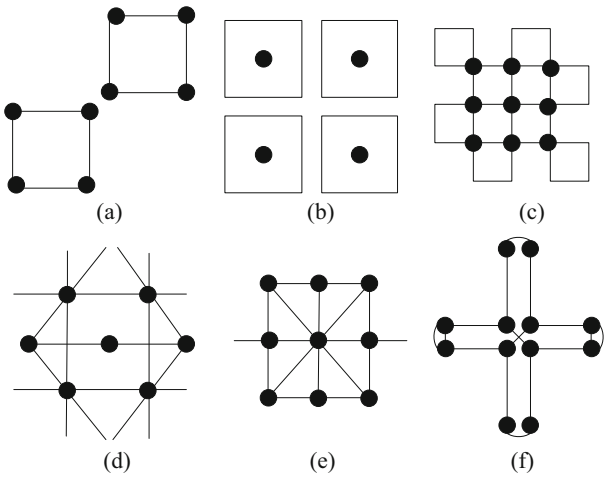

Fig. 1. Schematic diagram of power supply data feature types

From the above figure, it can be seen that there are many hidden layers of data and complex feature attributes. Therefore, the data output results in each hidden layer are calculated according to formula (4) and formula (5):

$$g(u,v) = K\left[\sum_{i=1}^{n} \delta_{ij}(U \times V) - \theta_j\right] \tag{6}$$

In the formula: $g(u,v)$ represents the amount of data output in the hidden layer within the dimensional value range of the data attribute; δ_{ij} represents the weight coefficient between the input layer i and the hidden layer j; θ_j represents the threshold in the hidden layer j. When the difference between the calculation result and the actual data value is greater than 0.3, it means that the data has an error and needs to be recalculated; when the calculated result is similar to the actual power data under the Internet of Things, it means that the amount of data obtained by the model is credible Yes, the data characteristics at this time are consistent with the actual situation.

2.3 Positioning Frequency Fluctuation Range Compressed Sensing Node Information

When users access the platform to obtain power information of electrical equipment, they are affected by network interference signals. Although the power information obtained has retrieval characteristics, it is scattered in the entire retrieval set. Considering the relevance and interactivity between network data transmission nodes, The network traffic transmission process is regarded as a movement process. The number of anchor nodes of the platform is known by default. When locating the range of feature data in the collection, assuming that the number, location and network topology of anchor nodes are fixed, set one of the target nodes to 0 and use n mobile anchor nodes to calculate location. Set the number of anchor nodes to $1, 2, \cdots, n$, one of the random nodes is i, the position is q_i, there is $q_i = \{q_{i,1}, q_{i,1}, \cdots, q_{i,m}\}$, where m represents the dimension of the network space, and $n \geq m+1$. Let the target node to be located be q_0, and calculate the distance between this node and other nodes. Using the idea of non-adjacent subtraction of the Internet of Things technology to eliminate the quadratic term in the multilateral positioning process. Assume that anchor node i needs to meet the following constraints:

$$l_{0,i} = \sqrt{\sum_{j=1}^{m} (q_{0,j} - q_{i,j})^2} \tag{7}$$

In the formula: $q_{0,j}$ represents the unknown variable to be determined. In order to facilitate the safe use of the Internet of Things technology, the above formula is transformed to obtain:

$$l_{0,j}^2 - \sum_{j=1}^{m} q_{i,j}^2 = \sum_{j=1}^{m} q_{0,j}^2 - 2\sum_{j=1}^{m} q_{0,j} q_{i,j} \tag{8}$$

According to the above conversion results, the n formula is used to subtract the i formula to eliminate the quadratic term on the left side of formula (8) to obtain a linear equation $Xq_0^T = Y$. According to the definition of X and Y in the formula, the linear equation estimation result:

$$\hat{q}_0^T = \left(X^T X\right)^{-1} X^T Y \tag{9}$$

The above results are the farthest distance of abnormal nodes in the Internet of Things with a target node as the center after calculation. Repeat the above steps to get the mining range consisting of all characteristic data in the set. The mining scope is shown in Fig. 2.

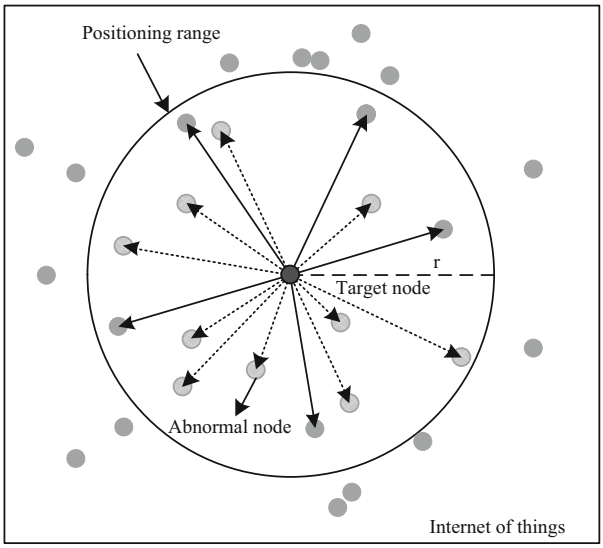

Fig. 2. Schematic diagram of positioning range

After the Internet of Things technology fully covers and senses the information link, information exchange and complete coverage as shown in Fig. 2 can be realized according to the changes of data characteristics of each node in the set. Then, through feature recognition of the nodes in the whole set, the range of the required power characteristic information node is located. After determining the range, a feature extraction method based on the sum of the distance between cluster centers is used to extract the abnormal node features due to the link failure. This process divides the obtained range into a training set and a test set, and then extracts k cluster centers from the training set, and then transforms the original m dimensional data set to obtain a brand-new k dimensional data set. The process consists of two main stages. The first stage is to cluster after the training set is obtained through the above method, and then extract the cluster center; the second stage is to calculate the sum of distances between the target node and each node again, so as to construct a new training set training data.

Suppose that after the k dimensional data set G is divided, the training set and the test set obtained are G_1 and G_2 respectively, and k unconnected clusters and cluster centers in G_1 are aggregated and extracted. Since the behavioral characteristics between nodes in the first stage are relatively similar, the data set needs to be divided into multiple clusters [9, 10]. Assuming that the data sample in G_1 is λ_i, calculate the distance between λ_i and all clusters, and obtain the closest cluster E_λ, repeat this step to obtain k cluster centers $e_1, e_2, \ldots, e_k$. The objective function at this time is:

$$\tau = \sum_{j=1}^{k} \sum_{i=1}^{n} \left\| \lambda_i^{(j)} - e_j \right\|^2 \tag{10}$$

In the formula: V is the distance measurement between the data sample $\lambda_i^{(j)}$ and the cluster center e_j of the cluster where it is located; $n < k$ represents the total amount of k dimensional data used. Through the above steps, k cluster centers in G_1 are obtained. Use G_1 and the cluster center to generate a k dimensional data set G_1', where each data sample is composed of the sum of k distances. According to the above analysis, the cluster center $e_1, e_2, \ldots, e_k$ is used to transform G_2 into a new data set G_2', and the classification algorithm is used to classify the result of G_2'. Given the distance within the positioning range, for any two data existing in the set, the relationship between the abnormal node and the abnormal edge node exists as shown in Fig. 3.

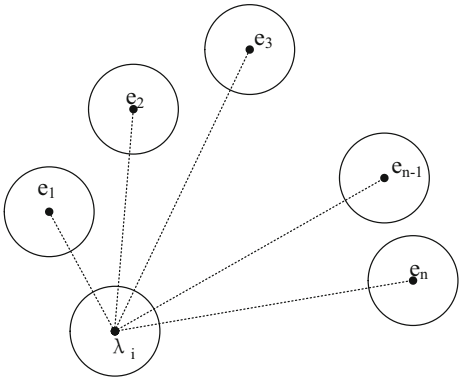

Fig. 3. Association between abnormal nodes and abnormal edge nodes

According to the mechanism shown in the figure, calculate the Euclidean distance between them, the formula is as follows:

$$dis(\lambda_i, e_j) = \sqrt{(\lambda_1 - e_1)^2 + \cdots + (\lambda_n - e_n)^2} \tag{11}$$

In the formula: n represents the number of abnormal nodes. By repeating the above calculation process, a new data set G_2' is obtained, and then node classification is performed to find out the strong and weak associations between multiple nodes and the

target node, and obtain the characteristics of all power data nodes with abnormal problems within the positioning range.

Among all the nodes obtained by positioning, the abnormal power information nodes are not evenly distributed. A distributed detection algorithm needs to be used to realize compressed sensing of all abnormal nodes, so as to realize the cyclic detection of retrieved data. The algorithm divides the entire positioning range into several subsets, and performs compressed sensing tasks in each subset. After the detection algorithm completes the loop detection work, the detection parameters are adjusted according to the detection results, and the corresponding detection matrix is adjusted at the same time [11]. Suppose the number of nodes in the positioning range is S, and $x(s), s = 1, 2, \ldots, S$ represents the discrete data vector. The detection algorithm performs a weighted tracking task for each location area, and uses the following formula to determine whether the data of each node exists because the link causes the characteristic value of the power supply to be abnormal:

$$F[x'(i)] = \begin{cases} \varphi_1 & if\ x'(i) > \beta, \forall i = 1, 2, \ldots, S \\ \varphi_0 & otherwise \end{cases} \tag{12}$$

In the formula: $x'(i)$ represents the i recovered data obtained after the algorithm weighted tracking; φ_1 represents the abnormality of the characteristic data node; φ_0 represents the abnormality of the characteristic data node; β represents the abnormal threshold of the node. Compare the calculation result with the actual situation, and adjust the regional weight of each positioning range. Summarize the detection situation of the entire collection, locate the detection result position from a global angle, and then adjust the detection matrix in the corresponding area. Here we assume that the set is divided into v sub-intervals, from which the detection model obtains b node information, and adjusts the number of detection nodes according to the following formula:

$$b_{ij} = b \times \frac{H_{ij}}{\sum_{i=1}^{v} H_{ij}} \tag{13}$$

In the formula: H_{ij} and H_{ij} respectively represent the number of data detections and the number of abnormal nodes found in the i subset during the j detection of the algorithm. The algorithm compresses and senses abnormal node information, so that the obtained electrical equipment power information characteristics are consistent with the retrieval target, and at the same time, the abnormal characteristic data of its own is removed to ensure that the control content is consistent with the target content.

2.4 Chaos Algorithm to Control Power Supply Frequency Fluctuation Trajectory

According to the characteristic parameters obtained above, the chaotic algorithm is used to track the fluctuation trajectory of the power frequency of the electrical equipment. The particle swarm optimization algorithm in the chaos algorithm finds the optimal solution for the particles in space through the way birds find food. Each particle

is used as a dimensional variable. Therefore, the general calculation equation of the chaotic particle algorithm is:

$$\begin{cases} \min L(\sigma) = L(\sigma_1, \sigma_2, \ldots, \sigma_n) \\ \sigma_{i\min} < \sigma_i < \sigma_{i\max}, i = 1, 2, \ldots, P \end{cases} \tag{14}$$

In the formula: σ_i represents the dimensional variable of the i particle; P represents the particle set. $L(\sigma)$ represents the result of particle swarm algorithm. Suppose that the i particle is denoted by T_i, and its most suitable value in the iterative process is T_0 by default. In the iterative process, the best particle produced in each generation is J_0, then the iterative formula of the chaotic particle swarm algorithm is:

$$\alpha_{ij}^{e+1} = \delta\alpha_{ij}^{e} + \kappa_1\varsigma_1\left(\alpha_{ij}^{e} - \sigma_{ij}^{e}\right) + \kappa_2\varsigma_2\left(J_{ij}^{e} - \sigma_{ij}^{e}\right) \tag{15}$$

In the formula: α_{ij}^{e} represents the j dimensional velocity of the i particle; δ represents the inertia factor; κ_1 and κ_2 are calculated by the matrix; ς_1 and ς_2 represent random numbers in the range; σ_{ij}^{e} represents the j dimension of the i particle variable. In the algorithm used in traditional control methods, as long as a particle is found closest to the optimal particle, the particle is regarded as the optimal particle. No matter whether there is a more suitable optimal solution later, the algorithm does not continue to iterate. The chaotic particle algorithm used this time uses the chaotic mapping method to map the particles into the solution space, while maintaining the diversity of the particles, it breaks through the defect of local optimization [12]. The Logistic mapping of the chaotic algorithm is the basic performance of a typical mapping. The initial equation of the mapping is:

$$f_{i+1} = \chi f_i(1 - f_i) \tag{16}$$

In the formula: χ represents a constant with a range between [3.57,4]; f_i represents the range of a chaotic sequence under Logistic mapping, with a value between (0,1). The logistic equation satisfies the traversal requirements of the chaotic algorithm. At this time, the power source signal source in the electrical equipment moves through all reachable and non-repetitive state points in the chaotic domain. Knowing the existence range of the chaotic sequence f_i, the variable value σ_i of the chaotic algorithm is mapped from the separate solution space to the chaotic sequence. Therefore, the calculation result of the comprehensive formula (14–16) is obtained, and the mapping equation of the chaotic variable is obtained as:

$$f_i = \frac{\sigma_i - \sigma_{i\min}}{\sigma_{i\max} - \sigma_{i\min}} \tag{17}$$

In the formula: $\sigma_{i\min}$ and $\sigma_{i\max}$ respectively represent the minimum and maximum values of the chaotic variable σ_i. According to the above calculation, the chaotic sequence mapping result is obtained and mapped to the variable value solution space of the algorithm, then:

$$\sigma_i = f_i(\sigma_{i\max} - \sigma_{i\min}) + \sigma_{i\min} \tag{18}$$

Logistic mapping is used to obtain the parameter values of the chaotic sequence particles, and the fluctuation trajectory of the power signal is tracked according to the results. This research requires the control of the power frequency of electrical equipment. Therefore, combining the premise that the sum of the three-phase current and the sum of the three-phase error current are zero, we get:

$$\Delta I_{ab} = -(\Delta I_{bc} + \Delta I_{ca}) \tag{19}$$

In the formula: ΔI_{ab}, ΔI_{bc}, and ΔI_{ca} respectively represent the error currents between phases *ab*, phase *bc*, and phase *ca*. Therefore, if the error current between the two phases can be controlled, and the phase is opposite, the third phase error current can be limited to the minimum range, thereby reducing the power loss of the electrical equipment. According to the variation of the error current, the controlled phase-to-phase error current requires fixed-frequency control. A standard reference frequency pulse is used as the control reference signal, and the phase of each phase switch is aligned with the reference signal to ensure that the phase switches can operate synchronously. In the initial stage of control, the proposed control method stabilizes the switching frequency in a fixed frequency range, and then fixes the phase difference between the switching phase and the standard pulse signal. When adjusting the frequency, a phase shift is used as the compensation for the hysteresis width [13]. By default, in the last switching cycle, the time difference between the midpoint of the 0-value signal and the pulse signal is Δc, then it is derived:

$$C = \left(\Delta c + \frac{R}{2R/C_2}\right) + \frac{R+r}{2R/C_1} + \frac{r}{2R/C_2} \tag{20}$$

In the formula: C represents the expected target of the switching signal level action time in the next cycle; C_1 and C_2 represent the high level and low level action time of the switching signal in the next cycle respectively[14]; R represents the current hysteresis width. Taking into account the compensation of the error current variation, assuming that the compensation is $\Delta\phi_1$ and $\Delta\phi_2$ respectively, the revised calculation result of formula (20) is:

$$C' = \left(\Delta c + \frac{R}{2R/C_2}\right) + \frac{R+r}{2R/C_1 + \Delta\phi_1} + \frac{r}{2R/C_2 + \Delta\phi_2} \tag{21}$$

In the formula: C' is the revised expected target under constant-frequency hysteresis current control [15]. According to the above process, the control of the power frequency of electrical equipment under the chaotic algorithm is realized.

3 Experimental Study

In order to further verify the control effect of the research method, the control method is applied to a simulation test environment, and a group of traditional control methods are used as a control group to compare the control differences between different methods. The experiment selects a certain electrical equipment in the power plant as the test object, uses simulation software to build a test environment, and sets the simulation experiment parameters shown in Table 1.

Table 1. Simulation experiment parameters

Serial number	Simulation parameters	Analog value
1	Air density	1.288 kg/m^3
2	Blade radius	1.85 m
3	Rated wind speed	12.8 m/s
4	Rated power	5.6 KW
5	Tip speed ratio	8.4
6	Wind energy coefficient	0.5
7	Running constant	0.0365
8	Moment of inertia	1.15 kg/m^2
9	Friction damping	0.05 N·s/rad
10	Number of pole pairs	5
11	Generator rated power	5.5 KW
12	Generator rated speed	585 r/min
13	Stator inductance	8.9 mH
14	Stator resistance	0.33 Ω
15	Main flux	0.35 × 10^{-3} Wb
16	Sliding mode controller parameters	0.01

According to the simulation parameters shown in Table 1, a test environment was established to test the control performance of the two methods. Figure 4 shows the changes in the electromagnetic torque, electromagnetic power, rotor angular speed and control signal of the generator's electromagnetic torque, electromagnetic power, rotor angular velocity and control signal after controlling the power frequency of the electrical equipment under the application of the two methods.

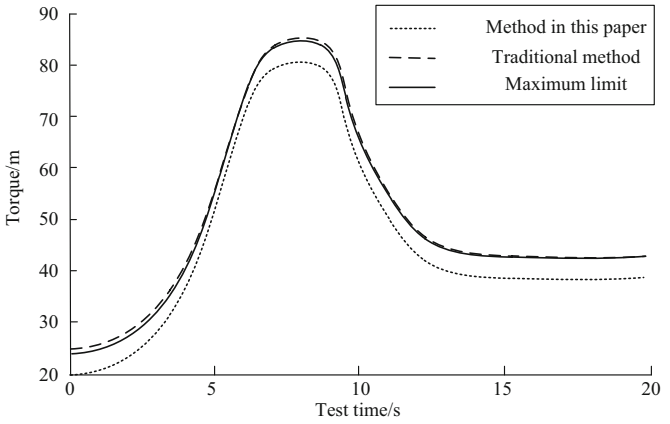

(a) Generator electromagnetic torque

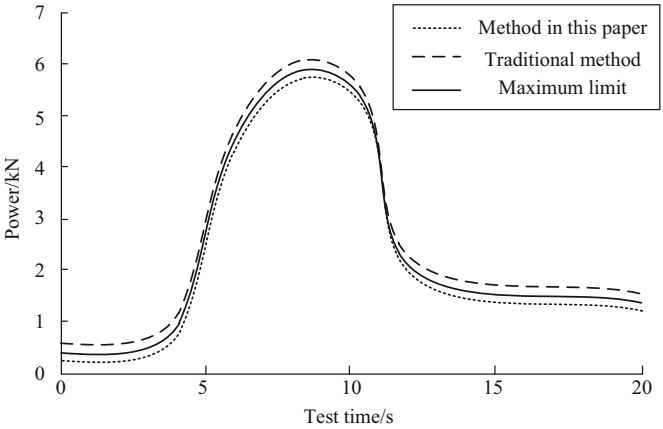

(b) Generator electromagnetic power

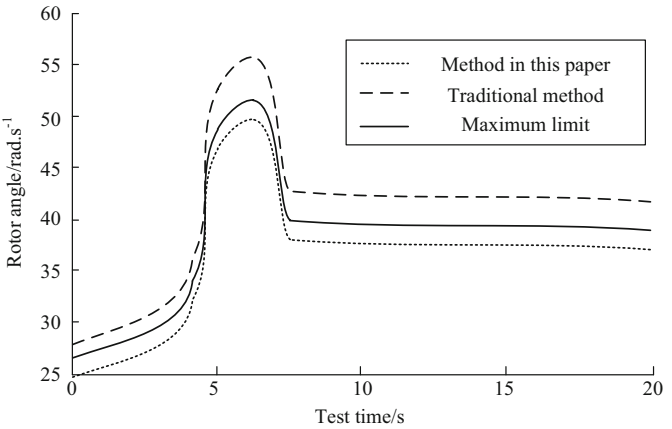

(c) Angular speed of generator rotor

Fig. 4. Control effect comparison test result

(b) Angular speed of generator rotor

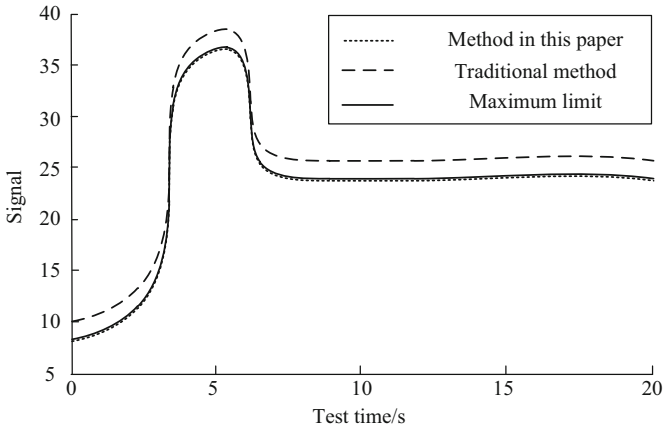

(d) Control signal

Fig. 4. (*continued*)

From the observation of the curves of the above four groups of test results, it can be seen that, on the basis of controlling the power supply frequency, the method in this paper accurately allocates data to the control center, so that the electromagnetic torque, electromagnetic power, rotor angular velocity and control signal of the generator of the entire electrical equipment are constrained within the limit value. However, the traditional method does not restrict the four parameters, which leads to the data overrun and brings great security risks for the use of electrical equipment.

In order to ensure the reliability of the test results, 10 rounds of testing were conducted for each group of tests, and AHP was used to evaluate the use safety of electrical equipment under four conditions. The evaluation results are shown in Table 2, Table 3, Table 4 and Table 5.

Table 2. Safety evaluation results for the use of electrical equipment (1)

Number of test rounds	Method in this paper	Traditional method
Round 1	0.9545	0.8863
Round 2	0.9536	0.8925
Round 3	0.9627	0.8842
Round 4	0.9548	0.8991
Round 5	0.9722	0.9036
Round 6	0.9716	0.8817
Round 7	0.9664	0.8988
Round 8	0.9582	0.8991
Round 9	0.9525	0.8865
Round 10	0.9817	0.8876
Average	0.9628	0.8919

Table 3. Safety evaluation results for the use of electrical equipment (2)

Number of test rounds	Method in this paper	Traditional method
Round 1	0.9721	0.8841
Round 2	0.9548	0.8743
Round 3	0.9725	0.8792
Round 4	0.9704	0.8786
Round 5	0.9636	0.8865
Round 6	0.9628	0.8892
Round 7	0.9714	0.8743
Round 8	0.9594	0.8907
Round 9	0.9545	0.8855
Round 10	0.9636	0.8628
Average	0.9645	0.8805

Table 4. Safety evaluation results of the use of electrical equipment (3)

Number of test rounds	Method in this paper	Traditional method
Round 1	0.9662	0.8584
Round 2	0.9701	0.8636
Round 3	0.9625	0.8427
Round 4	0.9488	0.8448
Round 5	0.9529	0.8533
Round 6	0.9443	0.8525
Round 7	0.9421	0.8672
Round 8	0.9557	0.8564
Round 9	0.9543	0.8565
Round 10	0.9625	0.8566
Average	0.9559	0.8552

Table 5. Safety evaluation results of use of electrical equipment (4)

Number of test rounds	Method in this paper	Traditional method
Round 1	0.9439	0.8763
Round 2	0.9488	0.8929
Round 3	0.9443	0.8876
Round 4	0.9447	0.8764
Round 5	0.9525	0.8852
Round 6	0.9546	0.8927
Round 7	0.9499	0.8914
Round 8	0.9476	0.8865
Round 9	0.9528	0.8829
Round 10	0.9537	0.8901
Average	0.9493	0.8862

This paper mainly analyzes the average safety factors in the above tables. Through data comparison, it can be found that the average safety factor of electrical equipment is 0.9581 after the application of the method in this paper. After the traditional method is applied, the average safety factor of electrical equipment is 0.8785, and there is a significant difference between the two. It can be seen that the method presented in this paper has a better control effect on the power frequency of the equipment and can effectively improve the safety of the equipment.

4 Conclusion

In this paper, a new power frequency control method for electrical equipment is proposed by combining Internet of Things technology, collaboration model, detection algorithm and chaos algorithm. This method firstly uses Internet of Things technology to collect power supply information of electrical equipment, and accurately extracts the frequency fluctuation characteristics of power supply, which lays a good foundation for subsequent control process. Then, by locating the frequency fluctuation range, accurate compressed sensing node information is obtained on the basis of two characteristic data processing. Then, chaotic algorithm is used to control the fluctuation trajectory of power frequency. The method has achieved success in the absorption stage, but it involves a lot of calculation process, so the efficiency of the method may be inferior to the traditional method. In the future, the calculation steps need to be simplified to improve the efficiency of the method.

Fund Projects. 2016 Guangxi Vocational Education Teaching Reform Project: Study on the Connection of Project Design between Specialized Courses in "Project Teaching" of Applied Electronic Technology Major in Higher Vocational Education, (GXGZJG2016B003).

References

1. Wang, Y., Zhou, Y., Yuan, X.: Study on high frequency ice-melting excitation source and control strategy. Electr. Meas. Instrument. **56**(10), 140–146 (2019)
2. Zhang, X., Wang, J.: Research on power system frequency control method considering power electronic interface. Electron. Test **15**(18), 30–31+83 (2020)
3. Xu, Z., Qin, H.: Design of intelligent light pole system based on IoT technology. Transd. Microsyst. Technol. **39**(06), 77–78+82 (2020)
4. Wu, J., Zhao, X., Zhao, J.: Modulation and demodulation of LoRa internet of things technology. Comput. Eng. Design **40**(03), 617–622 (2019)
5. Zheng, F., Dai, M., Chen, H.: Research on power cooperative control of multi-inverters for Power-Supply of microgrid. Comput. Simul. **36**(03), 137–141 (2019)
6. Sun, B., Tang, Y., Ye, L., et al.: Integrated frequency control strategy for wind power cluster with multiple temporal-spatial scale coordination based on H-DMPC. Proc. CSEE **39**(01), 155–167+330 (2019)
7. Liu, S., Sun, G., Fu, W.: e-Learning, e-Education, and Online Training, pp. 1–386. Springer, Boston (2018). https://doi.org/10.1007/978-3-030-63952-5

8. Chen, G., Li, Z., Guo, Y., et al.: Research on simulation of load frequency control for interconnected power grid based on Simulink. Exp. Technol. Manag. **36**(01), 124–129 (2019)
9. Liu, S.: Introduction of key problems in Long-Distance learning and training. Mob. Netw. Appl. **24**(01), 1–4 (2019)
10. Zhang, B., Tan, W., Li, J.: Tuning of linear active disturbance rejection control for load frequency control systems with hydro turbines. Electr. Mach. Control **23**(01), 117–124 (2019)
11. Li, X., Jia, H., Mu, Y., et al.: Coordinated frequency control based on electric vehicles and heat pumps considering time-delay. Electr. Power Autom. Equip. **40**(04), 88–95+110 (2020)
12. Liu, S., Liu, X., Wang, S., Khan, M.: Fuzzy-Aided solution for Out-of-View challenge in visual tracking under IoT assisted complex environment. Neural Comput. Appl. **33**(4), 1055–1065 (2021)
13. Chang, Y., Li, W., Ba, Y., et al.: A new method for frequency control performance assessment on operation security. Trans. China Electrotech. Soc. **34**(06), 1218–1229 (2019)
14. Xu, D., Wang, D.: resonance frequency tracking control of magnetic resonance wireless power transfer systems. Autom. Instrum. **17**(04), 20–24 (2020)
15. Zhao, Z., Meng, Z., Zhang, J., et al.: Control strategy of coordination and equalization for diesel generator and energy storage system in emergency microgrid. Autom. Electr. Power Syst. **43**(10), 53–59+141 (2019)